Original Article

Pan-cancer analysis of CXCR4 carcinogenesis in human tumors

Sen Wang[1], Lin Wang[2], Si-Wen Chen[3]

[1]School of Life Sciences, Shanxi University, Taiyuan, China; [2]School of Medicine, Nankai University, Tianjin, China; [3]Department of Gastroenterology, Second Medical Center, PLA General Hospital, Beijing, China

Contributions: (I) Conception and design: S Wang; (II) Administrative support: L Wang, SW Chen; (III) Provision of study materials or patients: S Wang, L Wang; (IV) Collection and assembly of data: S Wang; (V) Data analysis and interpretation: S Wang; (VI) Manuscript writing: All authors; (VII) Final approval of manuscript: All authors.

Correspondence to: Lin Wang. School of Medicine, Nankai University, Tianjin, China. Email: 2120191308@mail.nankai.edu.cn; Si-Wen Chen. Department of Gastroenterology, Second Medical Center, PLA General Hospital, Beijing, China. Email: chensiwenfj@126.com.

Background: C-X-C chemokine receptor 4 (CXCR4) is a specific receptor of stromal cell-derived factor-1, also known as CXCL12. The interaction between CXCL12 and its receptor CXCR4 can activate various signaling pathways, including gene expression, cell proliferation, migration, tumorigenesis, angiogenesis, etc. Although there is evidence to support the association between CXCR4 and some cancers, there is no pan-cancer analysis. To fill this gap, we analyzed the role of CXCR4 in cancer-based on The Cancer Genome Atlas (TCGA).

Methods: We used TCGA, Genotype-Tissue Expression (GTEx) and Clinical Proteomic Tumor Analysis Consortium (CPTAC) databases to analyze the expression, variation and phosphorylation of CXCR4 in different cancers. At the same time, we also carried out Kyoto Encyclopedia of Genes (KEGG) and Gene Ontology (GO) enrichment analysis.

Results: We found that *CXCR4* expression was significantly increased in bladder urothelial carcinoma (BLCA) and other cancers, and *CXCR4* expression in BLCA, cervical squamous cell carcinoma (CESC) and other cancers was related to tumor stage. *CXCR4* expression was positively correlated with tumor-associated fibroblasts in BLCA, breast adenocarcinoma (BRCA), CESC and other cancers. GO analysis showed that *CXCR4*-related genes were mainly enriched in biological processes (BPs) and cellular components (CCs). KEGG analysis showed that CXCR4 was mainly involved in "chemokine signaling pathway", "natural killer cell-mediated cytotoxicity", and "JAK-STAT signaling pathway".

Conclusions: The expression of *CXCR4* in different cancers has different effects on the prognosis of patients and the infiltration of immune cells.

Keywords: C-X-C chemokine receptor 4 (CXCR4); cancer; prognosis; gene; immune

Submitted Jul 27, 2021. Accepted for publication Sep 07, 2021.
doi: 10.21037/tcr-21-1561
View this article at: https://dx.doi.org/10.21037/tcr-21-1561

Introduction

With the development of science and medical technology, human mortality is gradually decreasing, while cancer mortality is increasing year by year. At present, people do not have a clear understanding of the occurrence and development of tumor, so it is very important to analyze the genes related to the occurrence and development of tumor and evaluate the relationship between these genes and clinical prognosis. Studies have shown that C-X-C chemokine receptor 4 (CXCR4), when binding to its ligand CXCL12, can affect the metastasis and invasion of some tumors (1). CXCL12 is a CXC chemokine, which is expressed in a variety of human tissues, including liver, lung, bone marrow, lymph nodes, stromal cells and so on (1). CXCR4 is a G-protein-coupled receptor, which can be expressed in various cells, including hematopoietic stem cells, stromal fibroblast satellite progenitor cells,

mesenchymal cells, lymphocytes, endothelial cells, epithelial cells, and germ cells (2,3). Through the human protein atlas (HPA) tool, we observed that *CXCR4* was expressed differently in different tissues, the highest in the thymus, followed by bone marrow and tonsil. However, *CXCR4* showed enhanced RNA tissue specificity in the bone marrow and lymphoid tissue.

At present, the structure and function of CXCR4 have been analyzed from the physiological and clinicopathological perspectives of varied species (3,4). The binding of CXCR4 and CXCL12 induces migration and invasion of cancer cells (5). Several drugs that block the binding of CXCR4 to CXCL12 have also passed the Food and Drug Administration (FDA) review (6). However, there is no pan-cancer analysis between CXCR4 and several types of cancer.

Here, we first use the data from The Cancer Genome Atlas (TCGA) database when we do the pan-cancer analysis of CXCR4. Meanwhile, the molecular mechanism of CXCR4 in the occurrence and development of cancer was also discussed in multiple aspects. It was concluded that there were differences between CXCR4 and prognosis in different tumor patients, and the relationship between CXCR4 and $CD8^+$ T cells or cancer-related fibroblast infiltration. These results provide a direction for the future research of CXCR4. We present the following article in accordance with the MDAR reporting checklist (available at https://dx.doi.org/10.21037/tcr-21-1561).

Methods

Genomic alterations of CXCR4 in cancers

The cBioPortal (http://cbioportal.org) tool can analyze the alteration of genes in different cancers and visualize the mutation types and sites. It can also be used for survival analysis associated with gene alterations, including overall survival (OS) and disease-free survival (DFS) rate. Then, it generated Kaplan-Meier plots with log-rank P value. Open the cBioPortal web, select "TCGA Pan Cancer Atlas Studies", and then click "Query by Gene" to input "CXCR4" to obtain the genetic alteration characteristics of CXCR4. The "Comparison/Survival" function was selected to obtain OS, DFS, progression-free survival (PFS), and disease-specific survival (DSS) of uterine corpus endometrial carcinoma (UCEC) and colon adenocarcinoma (COAD), cervical squamous cell carcinoma (CESC). All procedures performed in this study involving human participants were in accordance with the Declaration of Helsinki (as revised in 2013).

Expression analysis of CXCR4

Tumor immune estimation resource version 2 (TIMER2) website (http://timer.cistrome.org/) can analyze the expression of *CXCR4* in various cancers in the TCGA database. Wilcoxon test was used. For some tumors without normal tissue in the TCGA database, Gene Expression Profiling Interactive Analysis version 2 (GEPIA2) website (http://gepia2.cancer-pku.cn/#index) can combine TCGA and Genotype-Tissue Expression (GTEx) database, so that we cannot only analyze the expression of *CXCR4* in tumor tissue, but also analyze the normal part (7-9). When P value cut-off =0.01 and log2fold change (log2FC) cut-off =1, the significant difference of *CXCR4* expression between them was revealed. After defining the expression level of *CXCR4*, the violin plots of *CXCR4* expression at stage I–IV was obtained by the Pathological Stage Plot function of GEPIA2. We chose transformed expression data of log2 [per million transcripts (TPM) +1] for plotting. Next, we analyzed the protein phosphorylation level of CXCR4 using the Clinical Proteomic Tumor Analysis Consortium (CPTAC) dataset on the UALCAN website (http://ualcan.path.uab.edu/index.html).

Survival prognosis analysis

To explore the connection between *CXCR4* expression and prognosis, we used the "Survival Map" module of GEPIA2 for analysis. According to the cut-off, high and low cut-off values were both 50%. We got the high and the low expression group. Then, the significance plots of OS and DFS of CXCR4 were obtained. A log-rank test was used.

Immune infiltration

TIMER2 web is a comprehensive analysis tool that systematically analyzes the immune infiltration of several types of cancer. Using TIMER2, first, we analyzed the relationship between the infiltration of $CD8^+$ T cells and the expression of *CXCR4*; second, to better understand the relationship between the expression of *CXCR4* and other immune cells, we also analyzed the relationship between the infiltration of cancer-associated fibroblasts and the expression of *CXCR4*. Purity-adjusted Spearman's rank correlation test obtained the P and partial correlation (cor) values.

Construction of protein-protein interaction (PPI) networks

STRING website (https://string-db.org/) is an online search database for known PPI relationships, which can be used for functional enrichment analysis of PPI networks. After entering the STRING website, we input "CXCR4" and "Homo sapiens". Next, we select "full STRING network" from network type, select "evidence" from the meaning of network edges, select "experiments" from the active interaction sources, select "low confidence (0.150)" from the minimum required interaction score, and select "only 50 interactors" as the max number of interactors. We screened 50 experimentally validated CXCR4-bound proteins.

Gene enrichment analysis

GEPIA2 correlation analysis obtained some genes related to *CXCR4* expression. We selected the top 10 genes and *CXCR4* for paired gene Pearson correlation analysis. In addition, we used TIMER2 to generate the heat map of *CXCR4* and the top 10 genes. The heat map has the cor and P value in the purity-adjusted Spearman's rank correlation test.

To further determine the role of *CXCR4* in tumorigenesis, 50 genes in the PPI network and 100 genes related to *CXCR4* were combined and analyzed for Gene Ontology (GO) and Kyoto Encyclopedia of Genes and Genomes (KEGG) enrichment by database for annotation, visualization, and integrated discovery (DAVID). In this analysis, we used the R language software. Two-tailed P<0.05.

Results

CXCR4 genetic alteration

We used the cBioPortal database to analyze the alteration of *CXCR4*. It was found that *CXCR4* had the highest alteration frequency (>8%) in patients with lymphoid neoplasm diffuse large B-cell lymphoma (DLBC). In DLBC, uterine carcinosarcoma (UCS), lung squamous cell carcinoma (LUSC), CESC, colorectal adenocarcinoma, pancreas adenocarcinoma, bladder urothelial carcinoma (BLCA), lung adenocarcinoma (LUAD), invasive breast carcinoma, head and neck squamous cell carcinoma (HNSC), kidney renal clear cell carcinoma (KIRC), and brain lower-grade glioma (LGG), mutation frequency accounted for the highest proportion. In sarcoma (SARC), "amplification" is the primary type. In addition, *CXCR4* copy number deletion was found in all cases of mesothelioma (MESO), as shown in *Figure 1A*. The alteration sites, types, and cases of *CXCR4* are shown in *Figure 1B*. Among several types of alteration, a missense mutation is the primary type of genetic alteration. R334* mutation was detected in 1 case of CESC, 1 case of UCEC, and 1 case of COAD, and R334* mutation is likely oncogenic. Next, we investigated the association of *CXCR4* gene alteration, survival, and prognosis in cancer patients. According to the data in *Figure 1C*, we found no significant differences in OS, DSS, DFS, and PFS between *CXCR4*-altered and unaltered in CESC, UCEC, and COAD.

Expression of CXCR4

To determine whether *CXCR4* expression is related to cancer, we first analyzed *CXCR4* gene expression in TCGA cancers and normal tissues using TIMER2. As shown in *Figure 2A*, in comparison with the control group, the expression of *CXCR4* in BLCA, breast adenocarcinoma (BRCA), cholangiocarcinoma (CHOL), glioblastoma multiforme (GBM), HNSC, KIRC, kidney renal papillary carcinoma (KIRP), LUSC, skin cutaneous melanoma (SKCM), stomach adenocarcinoma (STAD) (P<0.001), pheochromocytoma and paraganglioma (PCPG) (P<0.01) and esophageal carcinoma (ESCA), pancreatic adenocarcinoma (PAAD), UCEC (P<0.05) were significant difference.

Since there are no normal tissues including acute myeloid leukemia (LAML) and LGG in the TCGA database, we use GEPIA2 to combine TCGA with the GTEx database to analyze LAML, LGG, ovarian serous cystadenocarcinoma (OV), testicular germ cell tumors (TGCT), and UCS. As shown in *Figure 2B*, CXCR4 was significantly different between tumor and normal tissues of LAML, LGG, OV, TGCT, and UCS (P<0.05). However, for other tumors, including adrenocortical carcinoma (ACC), DLBC, SARC, thymoma (THYM), no significant difference was found, as shown in Figure S1A.

Through GEPIA2, we observed that the expression of *CXCR4* in BLCA, CESC, LUAD, SKCM, STAD, thyroid carcinoma (THCA), UCS (*Figure 2C*) was correlated with pathological tumor staging, but there was no significant correlation for other tumors (Figure S1B). Using the CPTAC dataset, we compared the phosphorylation levels of CXCR4 between normal tissues and primary tumor tissues (10). In ovarian cancer, CXCR4 phosphorylation sites and significant differences are shown in *Figure 2D*. We found that the phosphorylation levels of S323, S325,

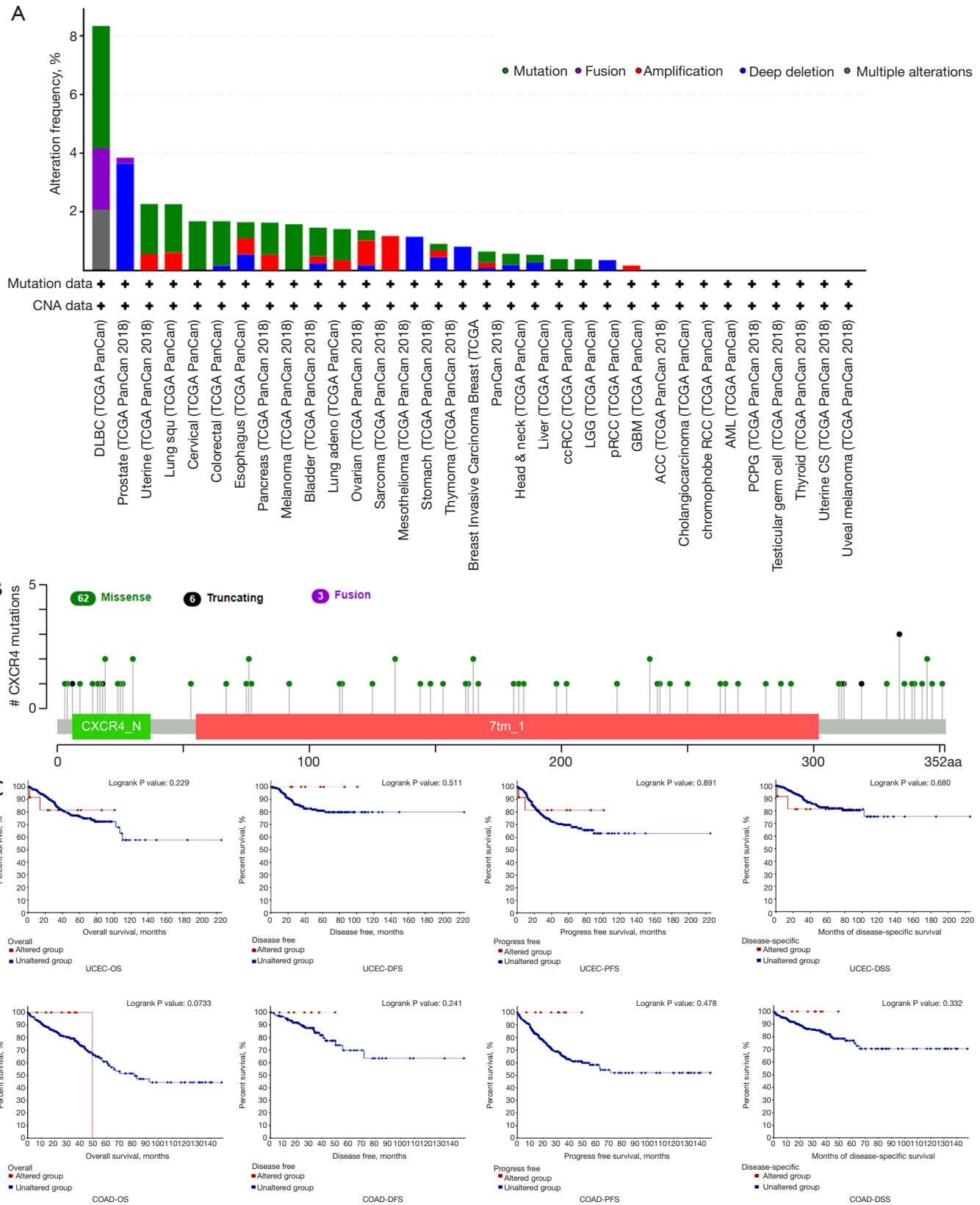

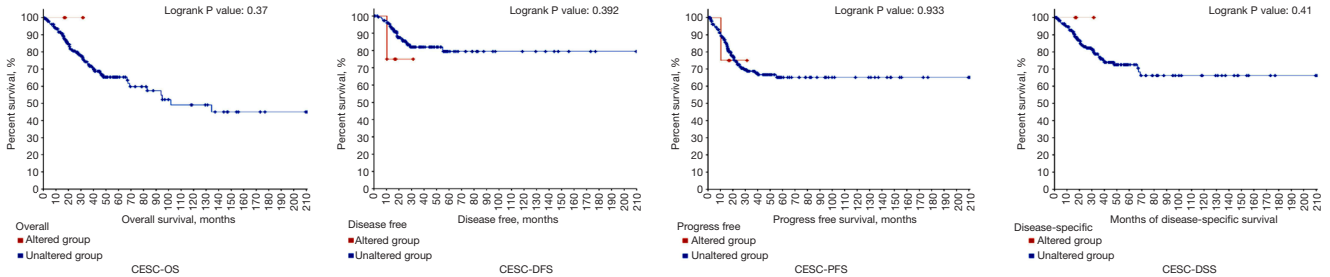

Figure 1 Mutation of *CXCR4*. The results of the cBioPortal tool analysis showed the relationship between *CXCR4* mutation type (A), mutation site (B), and mutation status (C) and OS, DSS, DFS, and PFS rates of patients with UCEC, COAD, and CESC. CXCR4, C-X-C chemokine receptor 4; OS, overall survival; DSS, disease-specific survival; DFS, disease-free survival; PFS, progression-free survival; UCEC, uterine corpus endometrial carcinoma; COAD, colon adenocarcinoma; CESC, cervical squamous cell carcinoma; TCGA, The Cancer Genome Atlas; CNA, copy number alteration; DLBC, diffuse large B-cell lymphoma; ccRCC, clear cell renal cell carcinoma; LGG, brain lower-grade glioma; pRCC, primary renal cell carcinoma; GBM, glioblastoma multiforme; ACC, adrenocortical carcinoma; AML, acute myeloid leukemia; PCPG, pheochromocytoma and paraganglioma; CS, carcinosarcoma.

and S343 of CXCR4 were increased in ovarian cancer compared to normal. There was a significant difference in phosphorylation between S323 and S343 (P<0.05) (*Figure 2E*). We also analyzed the phosphorylation of CXCR4 identified by CPTAC using the PhosphoNET database, and found phosphorylation at S325. This observation requires us to explore further the potential role of S323, S325, and S343 phosphorylation in tumorigenesis.

CXCR4 and prognosis

In the TCGA project, the increased expression of *CXCR4* is associated with poor OS prognosis for STAD (P=0.0067), UCS (P=0.0074), and uveal melanoma (UVM) (P=0.024), as shown in *Figure 3A*. In DFS, high *CXCR4* expression was associated with poor prognosis in patients with KIRC (P=0.014), UVM (P=0.0037), as shown in *Figure 3B*. In addition, low *CXCR4* expression was related to poor OS prognosis for OV (P=0.011), SKCM (P=0.021), and LUAD (P=0.049) (*Figure 3A*) and DFS prognosis for ESCA (*Figure 3B*, P=0.0055). The above data show that the expression of *CXCR4* differs from the prognosis of tumors.

CXCR4 and immune cell infiltration

Tumor immune cell infiltration is the movement of immune cells from the blood to the tumor tissue to perform their duties. Immune cell infiltration in the tumor is closely related to clinical outcomes. Using the TIMER2 tools, we evaluated the association between *CXCR4* expression and $CD8^+$ T cell and cancer-associated fibroblast infiltration using TIMER, XCELL, and other algorithms. In BRCA, BRCA-LumA, CESC, KIRC, MESO, PAAD, SKCM, and STAD, the infiltration of $CD8^+$ T-cells positively correlated with the expression of *CXCR4* (Figure S2). We also observed that *CXCR4* expression was positively correlated with cancer-associated fibroblast infiltration in BLCA, BRCA, BRCA-LumA, CESC, COAD, ESCA, HNSC, HNSC–human papillomavirus (HPV)–, KIRP, LGG, LIHC, LUAD, LUSC, PAAD, PCPG, prostate adenocarcinoma (PRAD), rectum adenocarcinoma (READ), STAD and THCA. However, there was a negative correlation in THYM (*Figure 4*). The scatter plot generated for the above tumors based on one algorithm is shown in *Figure 4B*.

PPI network

By using the STRING database, we build the PPI network of CXCR4. As shown in *Figure 5*, the PPI network has 51 nodes and 202 edges. All the 50 CXCR4-bound proteins were verified experimentally.

Gene enrichment results

The top 100 genes associated with *CXCR4* expression were obtained using the GEPIA2 tool. To understand the role of the *CXCR4* gene in tumor genesis and development, and its molecular mechanism, we performed GO and KEGG analysis on 50 CXCR4-binding proteins and 100 *CXCR4* expression-related genes. The *CXCR4* expression was correlated with *RASAL3* (R=0.54), *CYTIP* (R=0.52), *ITK*

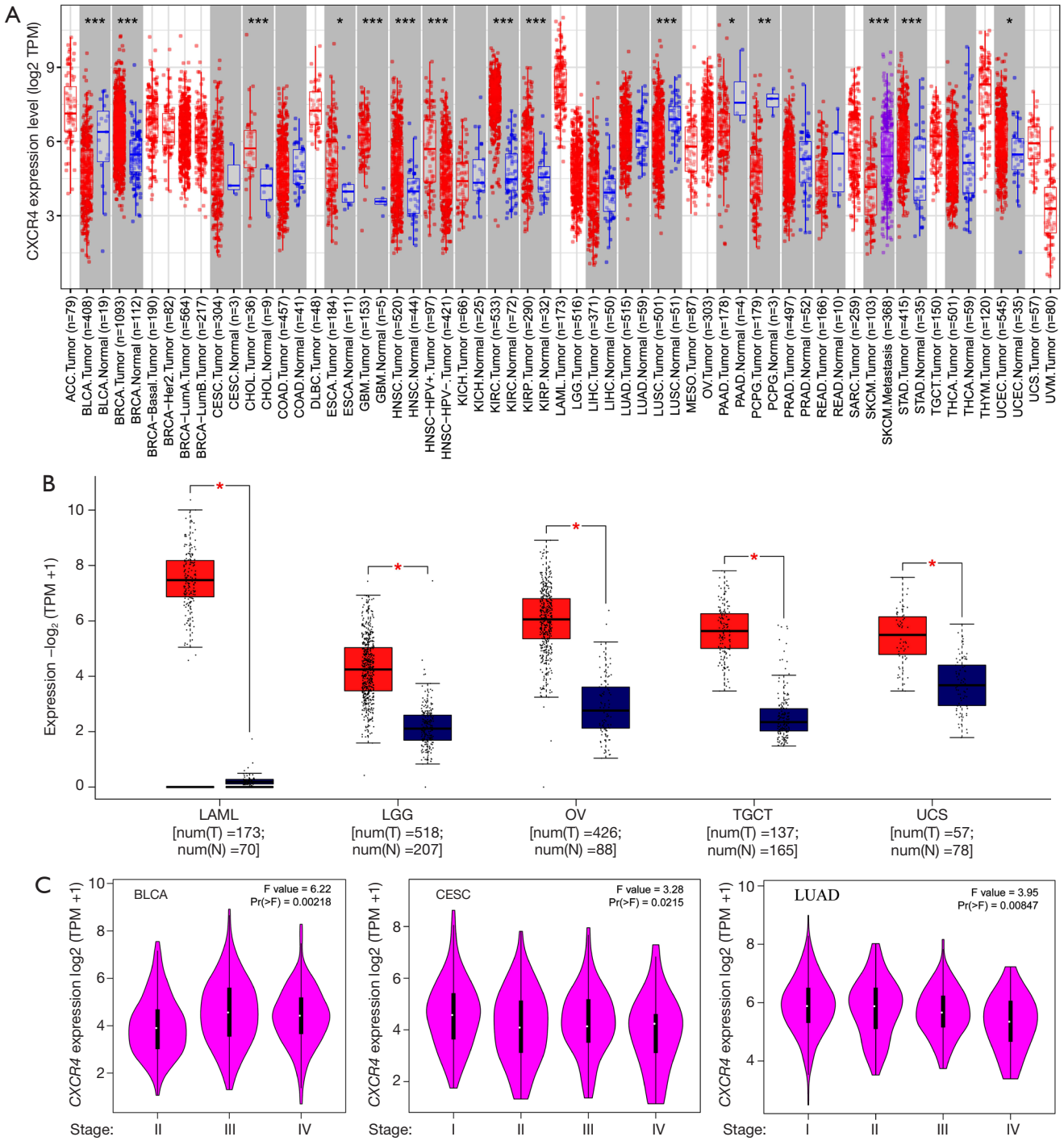

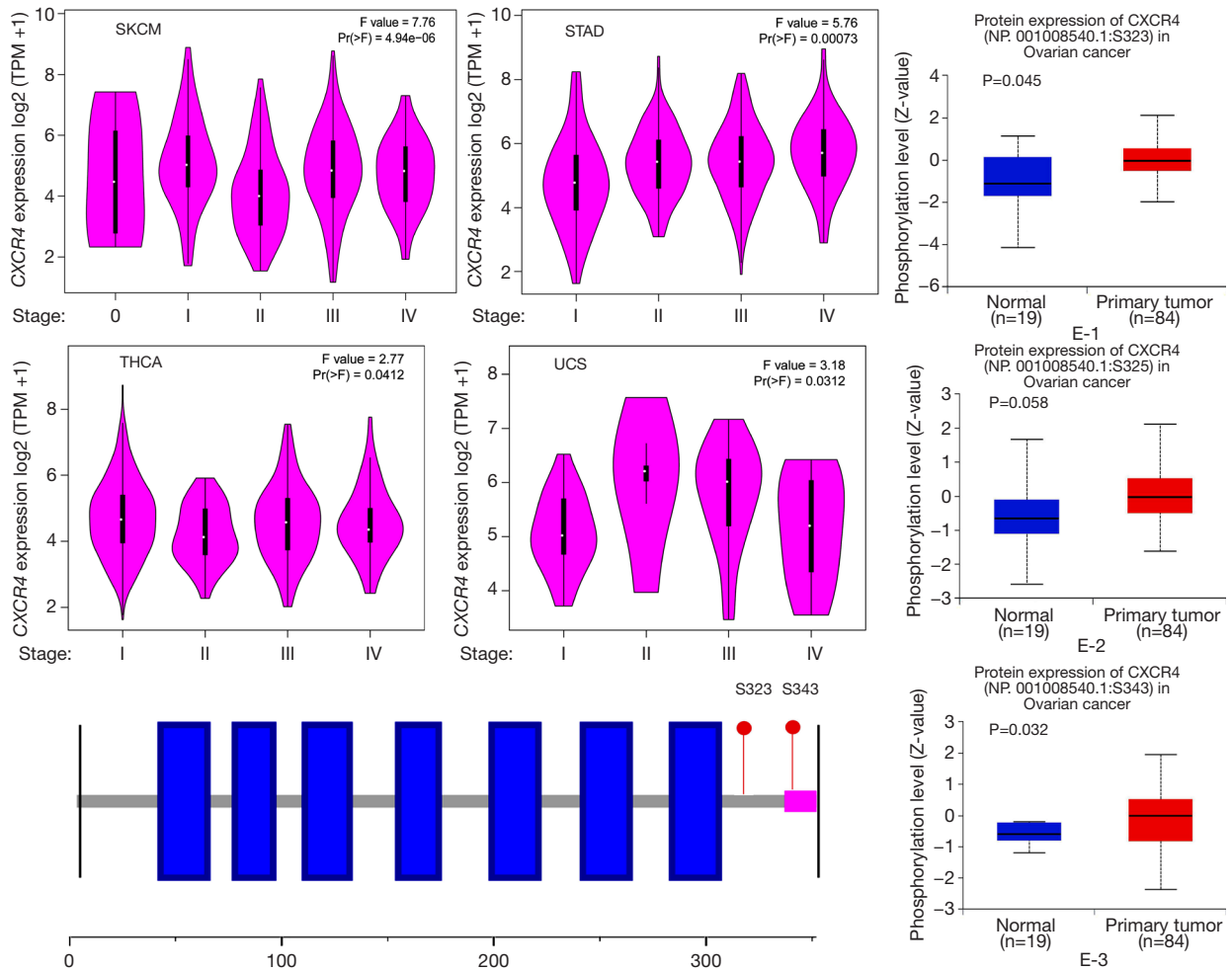

Figure 2 Expression of *CXCR4* and phosphorylation of CXCR4. (A) The expression of *CXCR4* in different cancers was determined using the TIMER2 tool. *, P<0.05; **, P<0.01; ***, P<0.001. (B) For LAML, LGG, OV, TGCT, and UCS, normal tissues from the GTEx database were used as controls. *, P<0.05. (C) TCGA data were used to analyze the expression of *CXCR4* in BLCA, CESC, LUAD, SKCM, STAD, THCA, and UCS at different pathological stages. (D) Phosphorylation sites of CXCR4 in ovarian cancer were analyzed using the UALCAN tool. (E) Phosphorylation of CXCR4 and expression of *CXCR4* at different sites in normal and primary tumor tissues. CXCR4, C-X-C chemokine receptor 4; TIMER2, tumor immune estimation resource version 2; GTEx, Genotype-Tissue Expression; TCGA, The Cancer Genome Atlas; ACC, adrenocortical carcinoma; BLCA, bladder urothelial carcinoma; BRCA, breast adenocarcinoma; CESC, cervical squamous cell carcinoma; CHOL, cholangiocarcinoma; COAD, colon adenocarcinoma; DLBC, diffuse large B-cell lymphoma; ESCA, esophageal carcinoma; GBM, glioblastoma multiforme; HNSC, head and neck squamous cell carcinoma; KICH, kidney chromophobe; KIRC, kidney renal clear cell carcinoma; KIRP, kidney renal papillary carcinoma; LAML, acute myeloid leukemia; LGG, brain low grade glioma; LIHC, liver hepatocellular carcinoma; LUAD, lung adenocarcinoma; LUSC, lung sauamous cell carcinoma; MESO, mesothelioma; OV, ovarian serous cystadenocarcinoma; PAAD, pancreatic adenocarcinoma; PCPG, pheochromocytoma and paraganglioma; PRAD, prostate adenocarcinoma; READ, rectum adenocarcinoma; SARC, sarcoma; SKCM, skin cutaneous melanoma; STAD, stomach adenocarcinoma; TGCT, testicular germ cell tumors; THCA, thyroid carcinoma; THYM, thymoma; UCEC, uterine corpus endometrial carcinoma; UCS, uterine carcinosarcoma; UVM, uveal melanoma.

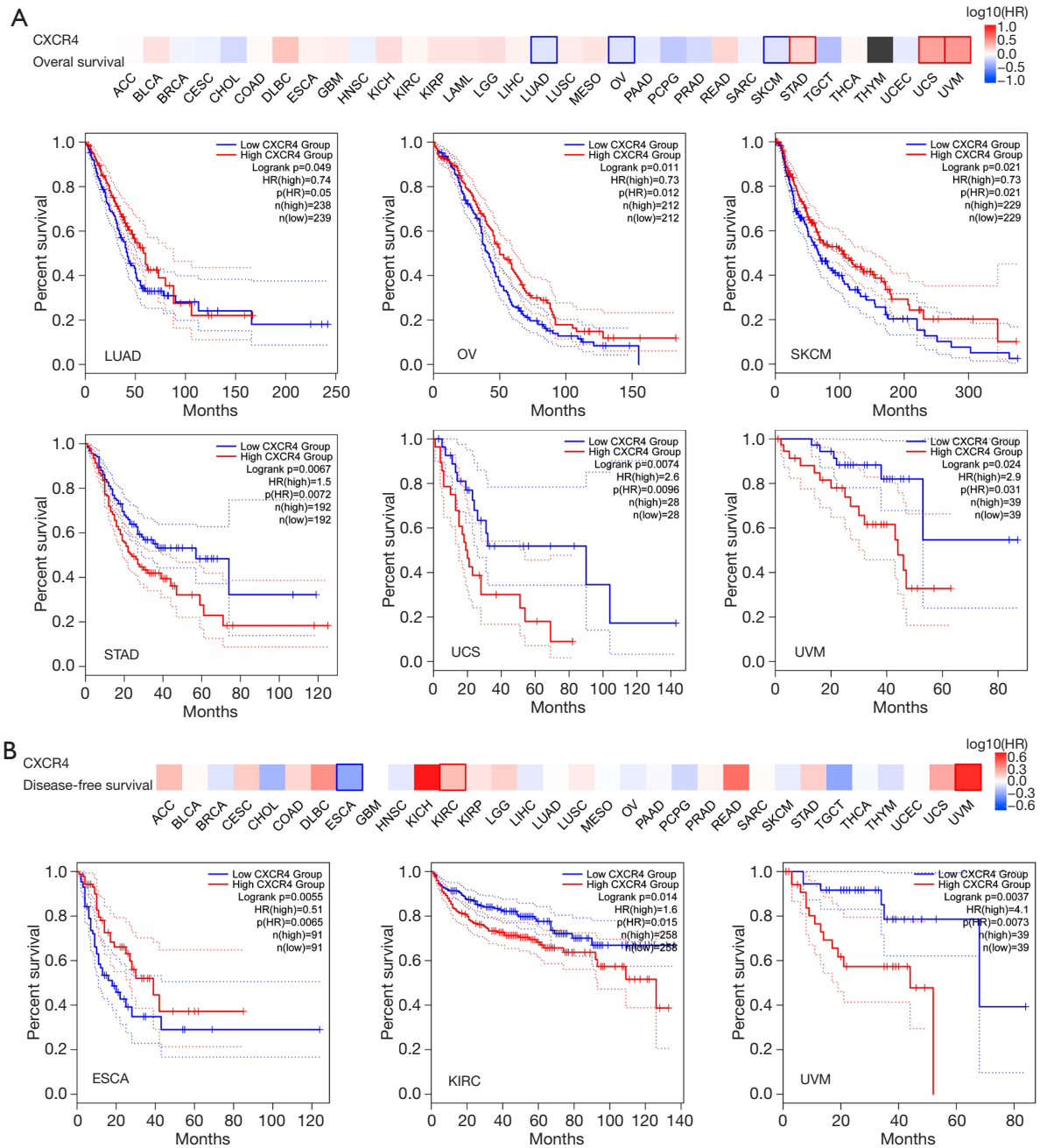

Figure 3 Relationship between *CXCR4* expression, patient survival, and prognosis. The OS (A) and DFS (B) associated with the expression of the *CXCR4* gene for different tumors were obtained using GEPIA2. CXCR4, C-X-C chemokine receptor 4; OS, overall survival; DFS, disease-free survival; GEPIA2, Gene Expression Profiling Interactive Analysis version 2; ACC, adrenocortical carcinoma; BLCA, bladder urothelial carcinoma; BRCA, breast adenocarcinoma; CESC, cervical squamous cell carcinoma; CHOL, cholangiocarcinoma; COAD, colon adenocarcinoma; DLBC, diffuse large B-cell lymphoma; ESCA, esophageal carcinoma; GBM, glioblastoma multiforme; HNSC, head and neck squamous cell carcinoma; KICH, kidney chromophobe; KIRC, kidney renal clear cell carcinoma; KIRP, kidney renal papillary carcinoma; LAML, acute myeloid leukemia; LGG, brain low grade glioma; LIHC, liver hepatocellular carcinoma; LUAD, lung adenocarcinoma; LUSC, lung sauamous cell carcinoma; MESO, mesothelioma; OV, ovarian serous cystadenocarcinoma; PAAD, pancreatic adenocarcinoma; PCPG, pheochromocytoma and paraganglioma; PRAD, prostate adenocarcinoma; READ, rectum adenocarcinoma; SARC, sarcoma; SKCM, skin cutaneous melanoma; STAD, stomach adenocarcinoma; TGCT, testicular germ cell tumors; THCA, thyroid carcinoma; THYM, thymoma; UCEC, uterine corpus endometrial carcinoma; UCS, uterine carcinosarcoma; UVM, uveal melanoma.

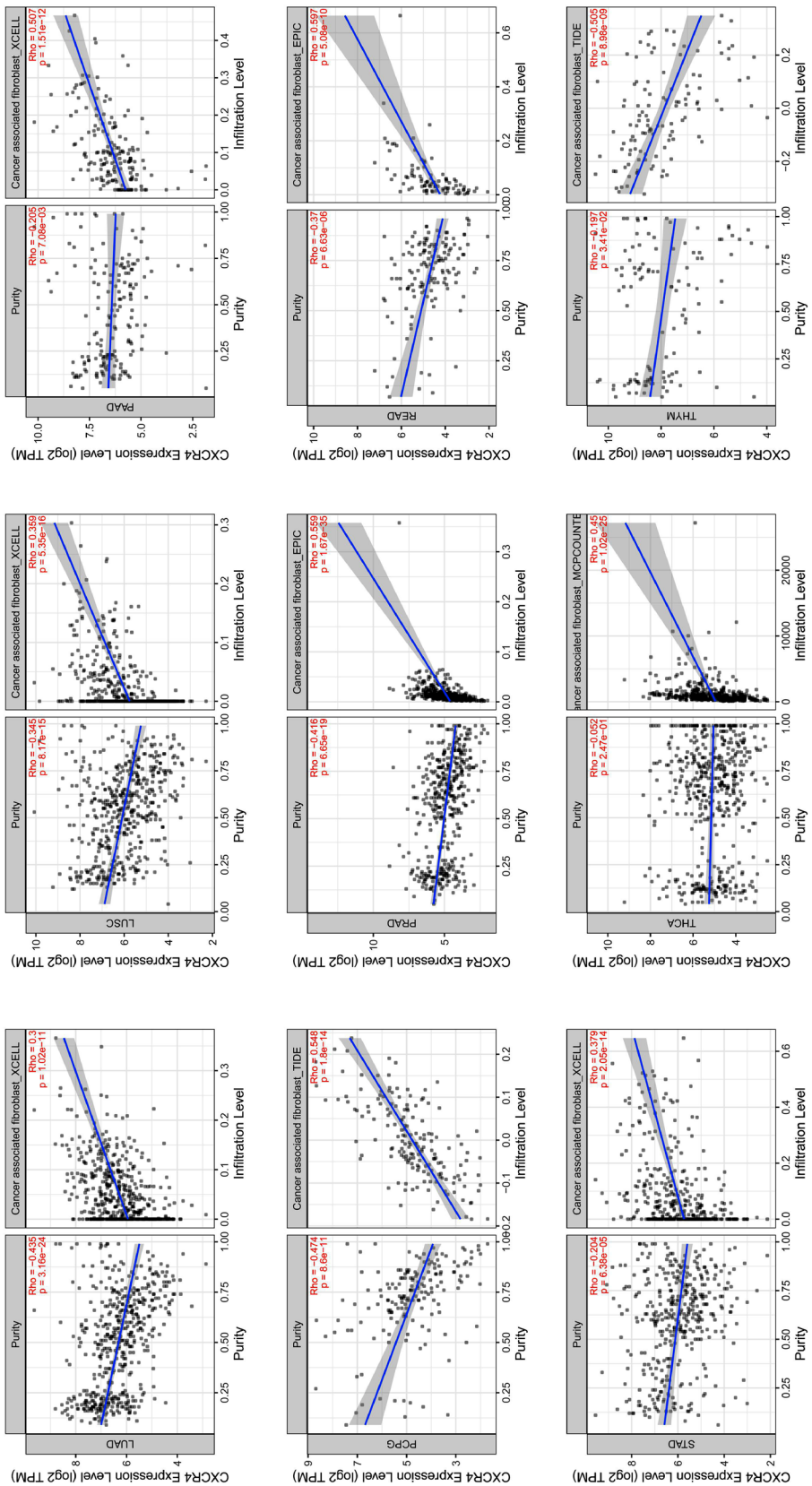

Figure 4 Analysis of the correlation between *CXCR4* expression and immune cells. (A) Correlation heat map between CXCR4 and cancer-associated fibroblast infiltration. (B) Scatter plot of correlation between CXCR4 and cancer-associated fibroblast infiltration. CXCR4, C-X-C chemokine receptor 4; ACC, adrenocortical carcinoma; BLCA, bladder urothelial carcinoma; BRCA, breast adenocarcinoma; CESC, cervical squamous cell carcinoma; CHOL, cholangiocarcinoma; COAD, colon adenocarcinoma; DLBC, diffuse large B-cell lymphoma; ESCA, esophageal carcinoma; GBM, glioblastoma multiforme; HNSC, head and neck squamous cell carcinoma; KICH, kidney chromophobe; KIRC, kidney renal clear cell carcinoma; KIRP, kidney renal papillary carcinoma; LGG, brain low grade glioma; LIHC, liver hepatocellular carcinoma; LUAD, lung adenocarcinoma; LUSC, lung squamous cell carcinoma; MESO, mesothelioma; OV, ovarian serous cystadenocarcinoma; PAAD, pancreatic adenocarcinoma; PCPG, pheochromocytoma and paraganglioma; PRAD, prostate adenocarcinoma; READ, rectum adenocarcinoma; SARC, sarcoma; SKCM, skin cutaneous melanoma; STAD, stomach adenocarcinoma; TGCT, testicular germ cell tumors; THCA, thyroid carcinoma; THYM, thymoma; UCEC, uterine corpus endometrial carcinoma; UCS, uterine carcinosarcoma; UVM, uveal melanoma.

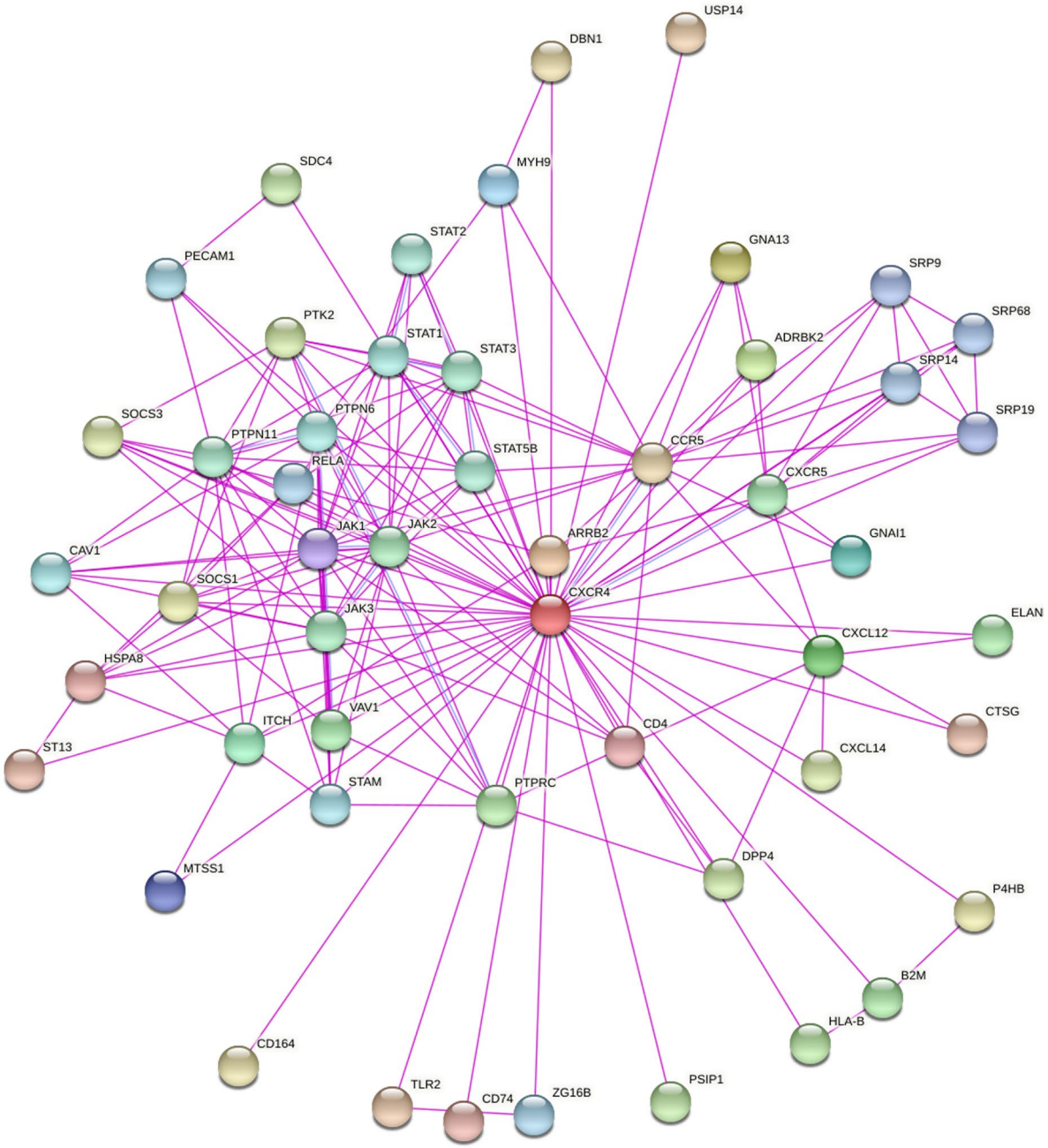

Figure 5 PPI network. PPI, protein-protein interaction.

(R=0.51), *VAV1* (R=0.51), *LCP2* (R=0.5), *PTPRC* (R=0.48), *TAGAP* (R=0.47), *SLA2* (R=0.47), *JAK3* (R=0.43), and *ARRB2* (R=0.35) positively correlated (all P<0.001), as shown in *Figure 6A*. According to the heatmap results, we also concluded that *CXCR4* was positively correlated with the above ten genes in most cancer types (*Figure 6B*). We used the Venn tool to analyze the above two groups of genes and found four common members, namely, *ARRB2*, *JAK3*, *PTPRC*, *VAV1* (*Figure 6C*) (11).

The results of GO analysis showed that these 146 genes were enriched primarily in biological processes (BPs) and cellular components (CCs), as shown in *Table 1*. The KEGG

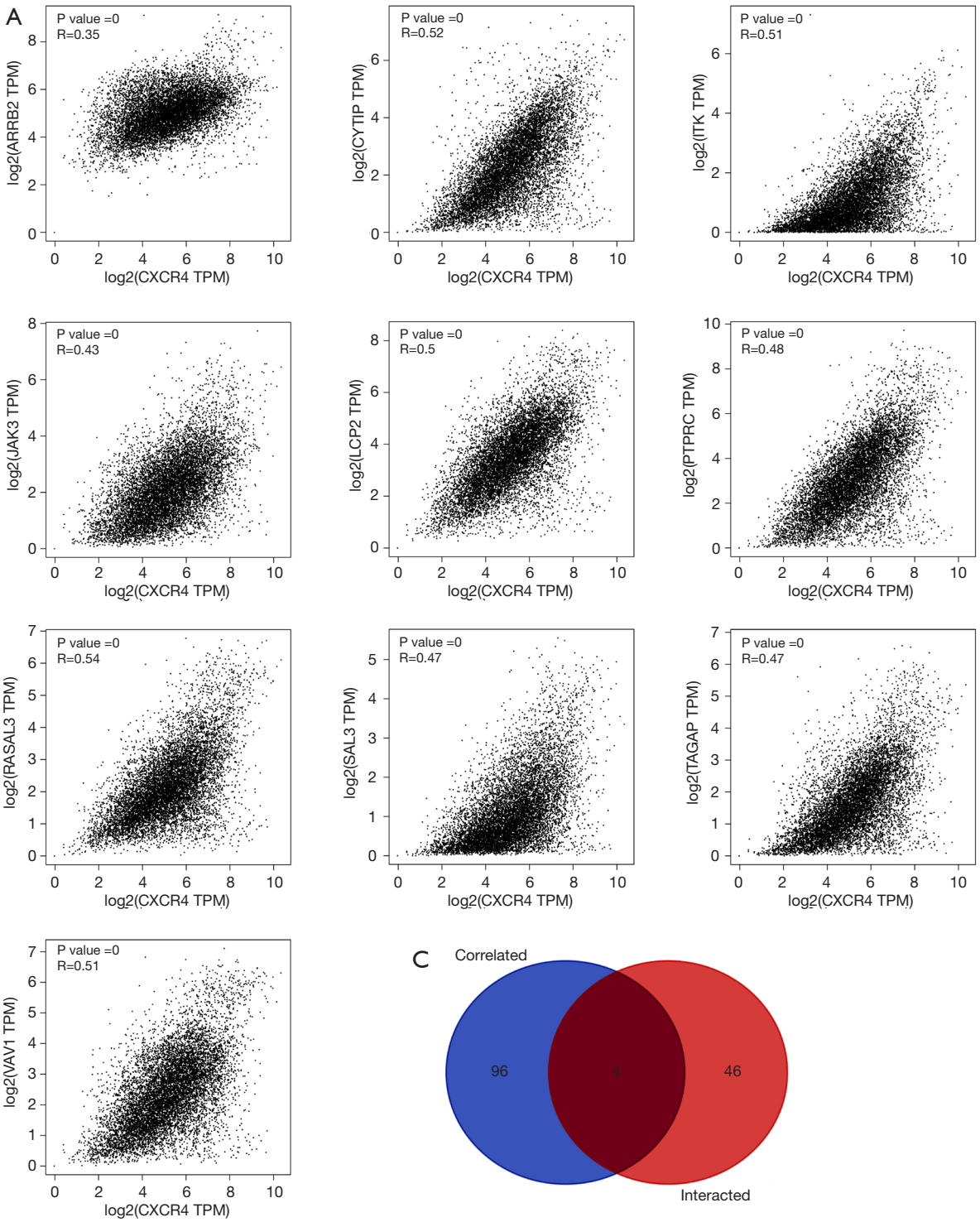

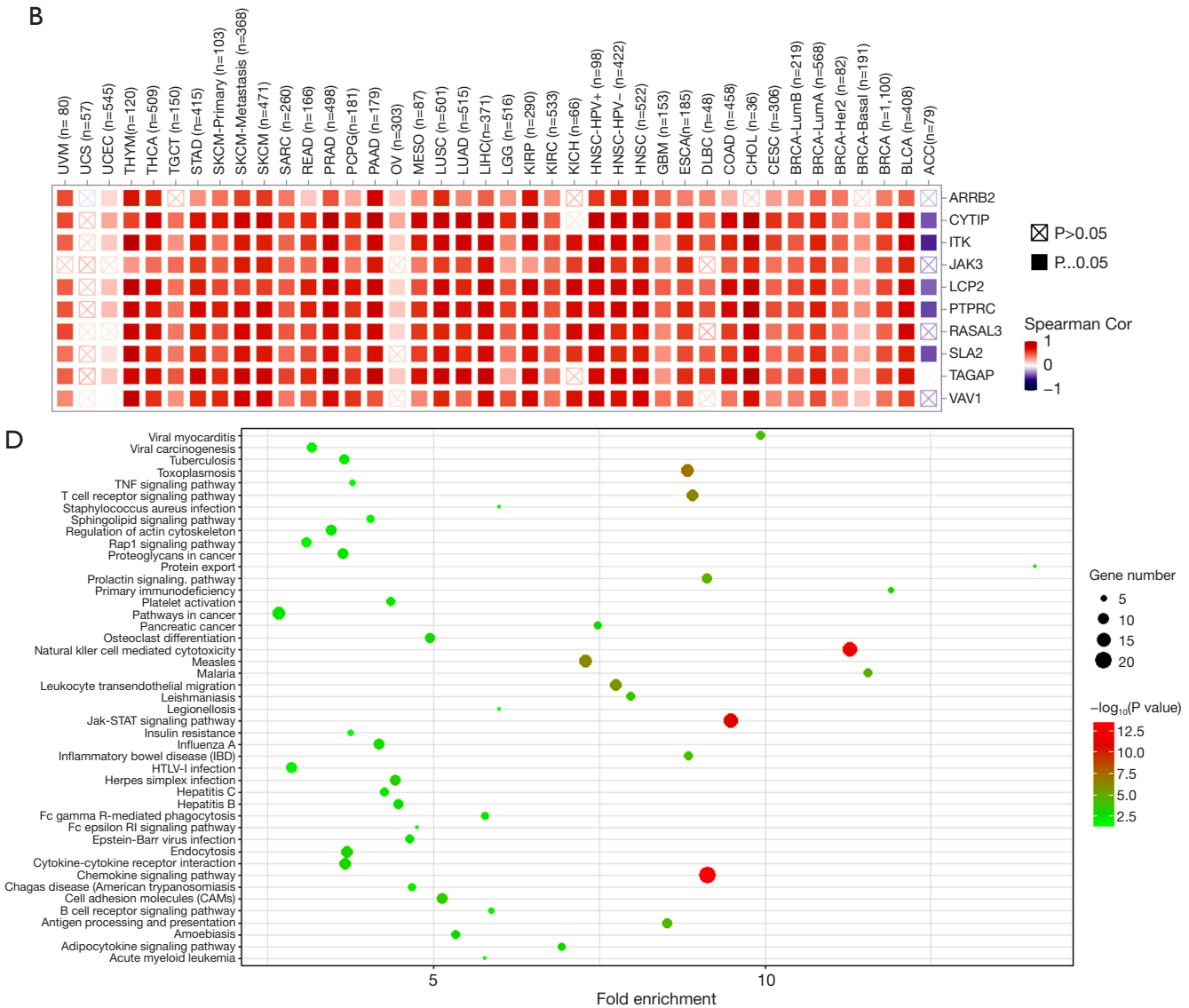

Figure 6 *CXCR4*-related gene enrichment analysis. (A) The top 100 *CXCR4*-related genes were identified using the GEPIA2 tool. Subsequently, the correlation between *CXCR4* expression and selected target genes (*ARRB2*, *CYTIP*, *ITK*, *JAK3*, *LCP2*, *PTPRC*, *RASAL3*, *SLA2*, *TAGAP*, and *VAV1*) were analyzed. (B) Heatmap of selected target genes and cancer types. (C) Cross analysis of CXCR4-binding genes and related genes. (D) KEGG pathway analysis of CXCR4-binding and interacting genes. CXCR4, C-X-C chemokine receptor 4; GEPIA2, Gene Expression Profiling Interactive Analysis version 2; KEGG, Kyoto Encyclopedia of Genes and Genomes; ACC, adrenocortical carcinoma; BLCA, bladder urothelial carcinoma; BRCA, breast adenocarcinoma; CESC, cervical squamous cell carcinoma; CHOL, cholangiocarcinoma; COAD, colon adenocarcinoma; DLBC, diffuse large B-cell lymphoma; ESCA, esophageal carcinoma; GBM, glioblastoma multiforme; HNSC, head and neck squamous cell carcinoma; KICH, kidney chromophobe; KIRC, kidney renal clear cell carcinoma; KIRP, kidney renal papillary carcinoma; LGG, brain low grade glioma; LIHC, liver hepatocellular carcinoma; LUAD, lung adenocarcinoma; LUSC, lung sauamous cell carcinoma; MESO, mesothelioma; OV, ovarian serous cystadenocarcinoma; PAAD, pancreatic adenocarcinoma; PCPG, pheochromocytoma and paraganglioma; PRAD, prostate adenocarcinoma; READ, rectum adenocarcinoma; SARC, sarcoma; SKCM, skin cutaneous melanoma; STAD, stomach adenocarcinoma; TGCT, testicular germ cell tumors; THCA, thyroid carcinoma; THYM, thymoma; UCEC, uterine corpus endometrial carcinoma; UCS, uterine carcinosarcoma; UVM, uveal melanoma.

Table 1 Enrichment results of the GO analysis

Category	Term	Description	Count	P value
BP	GO:0006955	Immune response	27	3.23E–14
BP	GO:0050776	Regulation of immune response	17	1.08E–10
BP	GO:0007165	Signal transduction	35	4.35E–10
BP	GO:0031295	T cell costimulation	10	1.28E–06
BP	GO:0045087	Innate immune response	17	1.58E–05
BP	GO:0006954	Inflammatory response	16	1.58E–05
BP	GO:0050900	Leukocyte migration	10	3.26E–05
BP	GO:0043547	Positive regulation of GTPase activity	17	2.92E–04
BP	GO:0007166	Cell surface receptor signaling pathway	10	0.006813328
BP	GO:0007155	Cell adhesion	11	0.044538617
CC	GO:0009897	External side of plasma membrane	16	5.21E–09
CC	GO:0005886	Plasma membrane	64	6.26E–09
CC	GO:0016020	Membrane	40	1.99E–06
CC	GO:0005829	Cytosol	49	1.29E–05
CC	GO:0005925	Focal adhesion	15	2.53E–05
CC	GO:0009986	Cell surface	17	4.24E–05
CC	GO:0045121	Membrane raft	11	5.10E–05
CC	GO:0005887	Integral component of plasma membrane	27	1.11E–04
CC	GO:0070062	Extracellular exosome	36	0.005446258
CC	GO:0005856	Cytoskeleton	10	0.013728634
MF	GO:0005515	Protein binding	96	2.66E–05
MF	GO:0005102	Receptor binding	15	5.35E–05
MF	GO:0005096	GTPase activator activity	11	0.002443655
MF	GO:0019901	Protein kinase binding	11	0.017081664

GO, Gene Ontology; BP, biological process; CC, cellular component; MF, molecular function.

data suggest CXCR4 may play a role in tumor development through the "chemokine signaling pathway", the "natural killer cell-mediated cytotoxicity", and the "JAK-STAT signaling pathway" (*Figure 6D*).

Discussion

A growing number of studies have shown a relationship between CXCR4 and clinical diseases, especially tumors (12). CXCR4 may take part in the occurrence and development of tumors through the same pathway, but this problem needs further study. By searching the published literature, we have not found any reports on the pan-cancer analysis of CXCR4. Therefore, using the data from TCGA and CPTAC databases, combined with the molecular characteristics of gene expression, gene mutation, or protein phosphorylation, we conducted a comprehensive analysis of the *CXCR4* gene from 33 tumors.

Compared with normal people, the expression of *CXCR4* was significantly different in LAML, LGG, OV and other tumors, but there was no significant change in ACC, DLBC and other tumors. Although there are significant differences in the expression of *CXCR4* in some tumors, the survival and prognosis analysis based on *CXCR4* gene has different

conclusions for different tumors.

After GO and KEGG analysis of 146 genes, we found that these genes were mainly concentrated in "chemokine signaling pathway", "natural killer cell-mediated cytotoxicity", and "JAK-STAT signaling pathway". We used multiple immune deconvolution methods to observe the expression of *CXCR4* in tumors and the $CD8^+$ T cell infiltration. Through observation, we found that the expression of *CXCR4* in BRCA, BRCA-LumA, CESC, KIRC, MESO, PAAD, SKCM, and STAD tumors was positively correlated with $CD8^+$ T cell immune infiltration. In some tumors, we also found that fibroblast infiltration was associated with *CXCR4* expression.

Based on the CPTAC data, we explored the role of CXCR4 in ovarian cancer from the perspective of protein. Our study shows that the CXCR4 at the S323 and S343 protein and phosphorylation levels in the primary tumors were higher than the normal controls. However, further investigations are needed to assess the potential role of CXCR4 phosphorylation at S323 and S343.

In this paper, we make it clear that the expression of *CXCR4* is indeed related to some cancers, and the expression level of *CXCR4* is related to the prognosis of some cancers. Maybe CXCR4 can be used as an indicator of the prognosis of these tumors. KEGG data show that CXCR4 may affect the occurrence and progression of cancer through "chemokine signaling pathway", "natural killer cell-mediated cytotoxicity", and "JAK-STAT signaling pathway". At the same time, we also found that *ARRB2*, *JAK3*, *PTPRC*, *VAV1* were involved in the expression of *CXCR4* and binding of CXCR4. According to our research, the future research on CXCR4 should mainly focus on the following aspects: (I) the relationship between *CXCR4* expression and prognosis; (II) what role does "chemokine signaling pathway", "natural killer cell-mediated cytotoxicity", and "JAK-STAT signaling pathway" play in the occurrence and development of cancer; (III) the relationship between *CXCR4* and *ARRB2*, *JAK3*, *PTPRC*, *VAV1*.

Acknowledgments

Funding: None.

Footnote

Reporting Checklist: The authors have completed the MDAR reporting checklist. Available at https://dx.doi.org/10.21037/tcr-21-1561

Conflicts of Interest: All authors have completed the ICMJE uniform disclosure form (available at https://dx.doi.org/10.21037/tcr-21-1561). The authors have no conflicts of interest to declare.

Ethical Statement: The authors are accountable for all aspects of the work in ensuring that questions related to the accuracy or integrity of any part of the work are appropriately investigated and resolved. All procedures performed in this study involving human participants were in accordance with the Declaration of Helsinki (as revised in 2013). Institutional ethical approval and informed consent were waived.

References

1. Bai T, Mai R, Ye J, et al. Circulating tumor cells and CXCR4 in the prognosis of hepatocellular carcinoma. Transl Cancer Res 2020;9:1384-94.
2. Zhou W, Guo S, Liu M, et al. Targeting CXCL12/CXCR4 axis in tumor immunotherapy. Curr Med Chem 2019;26:3026-41.
3. Wu B, Chien EY, Mol CD, et al. Structures of the CXCR4 chemokine GPCR with small-molecule and cyclic peptide antagonists. Science 2010;330:1066-71.
4. Kircher M, Herhaus P, Schottelius M, et al. CXCR4-directed theranostics in oncology and inflammation. Ann Nucl Med 2018;32:503-11.
5. Domanska UM, Kruizinga RC, Nagengast WB, et al. A review on CXCR4/CXCL12 axis in oncology: no place to hide. Eur J Cancer 2013;49:219-30.
6. Kawaguchi N, Zhang TT, Nakanishi T. Involvement of CXCR4 in normal and abnormal development. Cells 2019;8:185.
7. Blum A, Wang P, Zenklusen JC. SnapShot: TCGA-analyzed tumors. Cell 2018;173:530.

8. Tomczak K, Czerwińska P, Wiznerowicz M. The Cancer Genome Atlas (TCGA): an immeasurable source of knowledge. Contemp Oncol (Pozn) 2015;19:A68-77.
9. Clough E, Barrett T. The Gene Expression Omnibus Database. Methods Mol Biol 2016;1418:93-110.
10. Chen F, Chandrashekar DS, Varambally S, et al. Pan-cancer molecular subtypes revealed by mass-spectrometry-based proteomic characterization of more than 500 human cancers. Nat Commun 2019;10:5679.
11. Bardou P, Mariette J, Escudié F, et al. jvenn: an interactive Venn diagram viewer. BMC Bioinformatics 2014;15:293.
12. Huynh C, Dingemanse J, Meyer Zu Schwabedissen HE, et al. Relevance of the CXCR4/CXCR7-CXCL12 axis and its effect in pathophysiological conditions. Pharmacol Res 2020;161:105092.

(English Language Editor: J. Chapnick)

Cite this article as: Wang S, Wang L, Chen SW. Pan-cancer analysis of CXCR4 carcinogenesis in human tumors. Transl Cancer Res 2021;10(9):4180-4195. doi: 10.21037/tcr-21-1561

